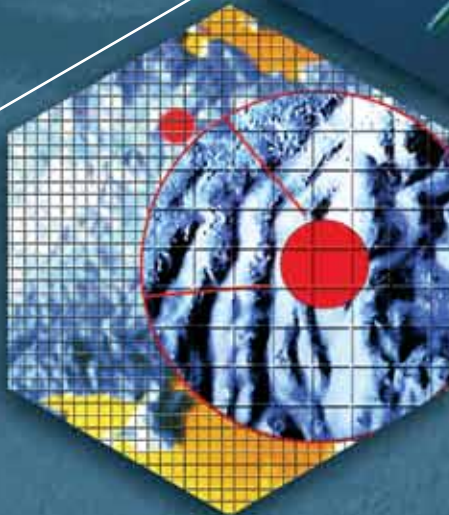


NOT FOR REPRODUCTION

REVIEWS & PAPERS



From the Technical Editor

Doing business at sea has always been risky. Storms can damage a ship or blow it off course. Mariners must always be vigilant, and keep a ‘weather eye’ out for any sight or sound of danger.



Another maritime threat is the danger caused by human intervention. Since the earliest days of human activity at sea, states have used it as a means of invasion. Other forms of violence at sea were also officially sanctioned. Until the middle of the 19th century, states condoned privateers, ‘authorized’ individuals who were free to plunder the ships of an enemy state. In addition, pirates used the high seas as a means for gathering their own wealth. Modern culture portrays pirates as the ultimate free-wheeling capitalists who were a band of brothers with their own code of conduct. In an ironic way, pirates were a symmetrical threat to their prey. Single ships were overcome in a winner-take-all battle of wits.

Modern pirates, such as those off the coast of Somalia, are now fighting a very asymmetrical battle, aided by modern technology. These pirates are heavily armed with highly portable but powerful weapons. They use small, fast boats to board large, relatively slow moving cargo vessels. The crew is overpowered and the ship, cargo and crew are held for ransom. As always, this is a profitable venture for the pirates, but how long will the world tolerate this disruption to trade, and how will we stop it? Will merchant ships be permitted to carry weapons to prevent them being boarded? Can radar and other sensors be enhanced to improve surveillance of small, fast attackers who can easily blend into legitimate activity? Can ships be managed differently so that they are better protected? For example, convoys were used in World War II as a way to combat the asymmetrical threat from German U-Boats against surface ships.

Although pirates enjoy some degree of protection, if they are caught in international waters, it is unlikely that they will be allowed to operate unchecked for very long. In the past, pirates were forced out of business by capture or changes in relationships which saw enemies become trading partners and the creation of states in previously stateless areas with the subsequent need for legitimate economic activity. It is likely that these changes will overcome modern pirates too, and there will not be much opportunity for technology to have an impact on the problem. After all, both sides have used technology to get where they are now and escalation of technology will likely just make the problems worse. In the end, if it is as profitable to work within the law as outside of it, then legitimacy will eventually win.

Dr. David Molyneux
Technical Editor

Getting to the bottom of things



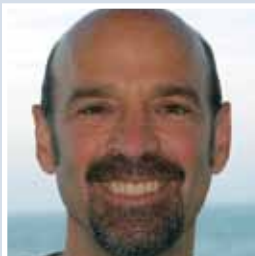
Paul McGill



Alana Sherman



Brett Hobson



Richard Henthorn



Ken Smith

McGill, Sherman, Hobson, Henthorn and Smith describe a new mobile platform for monitoring sedimentary processes in the deep ocean.

Who should read this paper?

Anyone with an interest in the challenges associated with engineering and deployment of deep sea instrumentation will find this paper interesting. In addition, deep sea scientists and others with an interest in sampling the deep ocean floor will be intrigued by the possibilities presented by the Rover.

Why is it important?

This paper describes the Rover, a new platform for long-term observations at abyssal depths. This is the only platform that the authors are aware of that is capable of making continuous time-series measurements of sediment community oxygen consumption at 6000 m depths for periods exceeding six months.

Continuous time-series measurements of sediment community oxygen consumption (SCOC) are critical to understanding the cycling of carbon in the deep ocean. Such measurements provide an estimate of the demand for organic carbon by the benthic community which the authors hypothesize will vary with changes in food supply from surface waters influenced by global warming. Long time-series measurements of SCOC are necessary to resolve short-term seasonal and episodic changes from long-term changes due to climate.

There is considerable interest in the oceanographic community to build similar benthic instruments to deploy on proposed cabled observatories worldwide. The Rover could also serve as a long-term mobile platform for monitoring impacts of deep-sea drilling and mining operations.

About the authors

Paul McGill is an Electrical Engineer with expertise in instrumentation, ocean observatories, and seafloor cabled networks.

Alana Sherman is an Electrical Engineer with an interest in scientific instrumentation, autonomous vehicles, and seafloor imaging systems.

Brett Hobson is a Mechanical Engineer whose focus is primarily on mobile platforms like the Rover and AUVs.

Richard Henthorn is a Software Engineer developing systems for autonomous vehicles and deep ocean platforms.

Ken Smith is a Senior Scientist studying the effects of climate change and food supply on deep-sea communities.

INITIAL DEPLOYMENTS OF THE ROVER, AN AUTONOMOUS BOTTOM-TRANSECTING INSTRUMENT PLATFORM

P.R. McGill, A.D. Sherman, B.W. Hobson, R.G. Henthorn, K.L. Smith, Jr.

Monterey Bay Aquarium Research Institute, Moss Landing, California, USA

www.mbari.org

ABSTRACT

The Benthic Rover is a bottom-transecting, autonomous vehicle currently in development at the Monterey Bay Aquarium Research Institute (MBARI), building on the earlier work of Smith and associates at the Scripps Institution of Oceanography. The Rover will be capable of making continuous time-series measurements at abyssal depths up to 6000 m for periods exceeding six months. Core instruments include two respirometer chambers for measuring sediment community oxygen consumption. Three cameras provide close-up images of the sediment surface and a wide-angle view of the Rover's immediate surroundings. A compass and a current meter allow the Rover to move when the current is coming from the desired direction of travel, thus preventing sediment clouds from disturbing the area to be studied. An onboard acoustic modem sends Rover status to surface ships, and receives instructions to change the mission or to terminate the deployment and return to the surface.

The vehicle weighs 68 kg in water and moves on two wide tracks with a combined surface contact area of about one square metre to provide good traction while minimizing the disturbance to benthic sediments. At the end of a mission, the vehicle releases a 113 kg steel drop weight to return to the surface.

A pair of 10 kWh lithium batteries will power the Rover for extended autonomous deployments. For engineering tests, typically lasting up to a few weeks, much less expensive alkaline battery packs are used. The Rover can also be powered by the Monterey Accelerated Research System (MARS) cable for testing in Monterey Bay at 900 m depth. In addition to power, the MARS cable provides communication capabilities enabling remote control capability and real-time access to Rover data and images, greatly aiding in the development of the autonomous software.

Engineering field tests have been performed with the Rover in Monterey Bay (900 m depth), and at Station M, 220 km west of the central California coast (4100 m depth). Rover operations have been observed with the ROVs *Ventana* and *Tiburon*, and with the manned submersible DSV *Alvin*. Knowledge gained from these engineering deployments has resulted in numerous modifications and improvements to the Rover.

INTRODUCTION

Coupling between a pelagically derived food supply and sediment community utilization of organic matter is critical to an understanding of biogeochemical cycling in the ocean [Smith et al., 2002; Smith and Kaufmann, 1999]. To resolve the coupling between pelagic and benthic systems, it is important to monitor the arrival and residence of organic matter on the sea floor using instrumentation capable of making measurements with appropriate spatial and temporal resolution. Critical questions which must be addressed to ultimately resolve pelagic-benthic coupling in the context of biogeochemical cycling are: 1) what is the quality and quantity of phytodetritus reaching the sea floor, and 2) what responses are elicited in the sediment community by the arrival of fresh detritus on the sea floor?

To address such critical questions, we developed a new autonomous bottom-transecting instrument, based on the original Rover design [Smith et al., 1997], to make long time-series estimates of fresh phytodetritus arriving on the sea floor. The Rover will be capable of conducting non-invasive time-series measurements of phytopigment fluorescence as an indicator of fresh phytodetritus on the sediment surface. Sediment community metabolism measurements (e.g. sediment community oxygen consumption) will be conducted on the same sediments along transects including up to fifty sites without docking, recharging, or data download.

Previous *in situ* measurements of sediment community metabolism were made with instruments deployed using either manned

submersibles, remotely operated vehicles (ROVs), or autonomous platforms yielding a measurement at a single location and time [Smith and Baldwin, 1983; Tengberg et al., 2005]. By taking measurements at multiple locations on a single deployment, the original Rover [Smith et al., 1997] represented a significant improvement in the temporal and spatial extent, as well as the cost-effectiveness, of such measurements. Now further development of this bottom-transecting instrument to include time-series measurements of phytopigment fluorescence combined with sediment community metabolism adds a significant improvement for analyzing time-series coupling between pelagic and benthic processes in the deep ocean.

MISSION PROFILE

From on board a research vessel, the Rover is deployed by crane into the water and freefalls to the ocean bottom. While waiting for disturbed sediment to settle, the Rover monitors the direction of the prevailing current in order to move into or across current to avoid contamination of measurement sites by suspended sediment carried down current. The direction of movement is programmed before deployment and remains the same throughout the mission to prevent the Rover from crossing its own tracks. Once the current is coming from an acceptable direction, the vehicle moves forward 10 metres to the first measurement site, where it again waits to allow disturbed sediments to settle down current and away from the study area. During the transit, a forward-looking survey camera captures images of the sediment surface. After movement stops and sediment has settled, two other cameras capture close-up optical images

of the study site, and an imaging fluorometer (currently in development) will record the quantity and distribution of phytodetritus on the sediment. Next, two benthic respirometer chambers are inserted approximately 2 cm into the sediment one at a time. The chambers contain optodes to measure sediment community oxygen consumption (SCOC), and will gather data for up to three days. After that time the chambers are raised and cleaned by water jets. The Rover then moves 10 m to a new study site and begins a new measurement cycle, repeating the sequence up to fifty times.

The Rover is recovered by sending a signal from a surface vessel, via an acoustic modem, telling the Rover to release a 113 kg drop

weight. This causes the Rover to float to the surface, where it is captured by crane and brought back on board (Figure 1).

The Rover is currently in development and has been deployed on eighteen test missions as of November 2008. The longest mission has been 16 days, but missions with fifty measurement sites may last greater than six months.

VEHICLE DESIGN

Mechanical Design

The mechanical configuration of the Rover is driven by multiple requirements: it must withstand depths of 6000 m; it must transit across very soft, sticky sediment; and it must

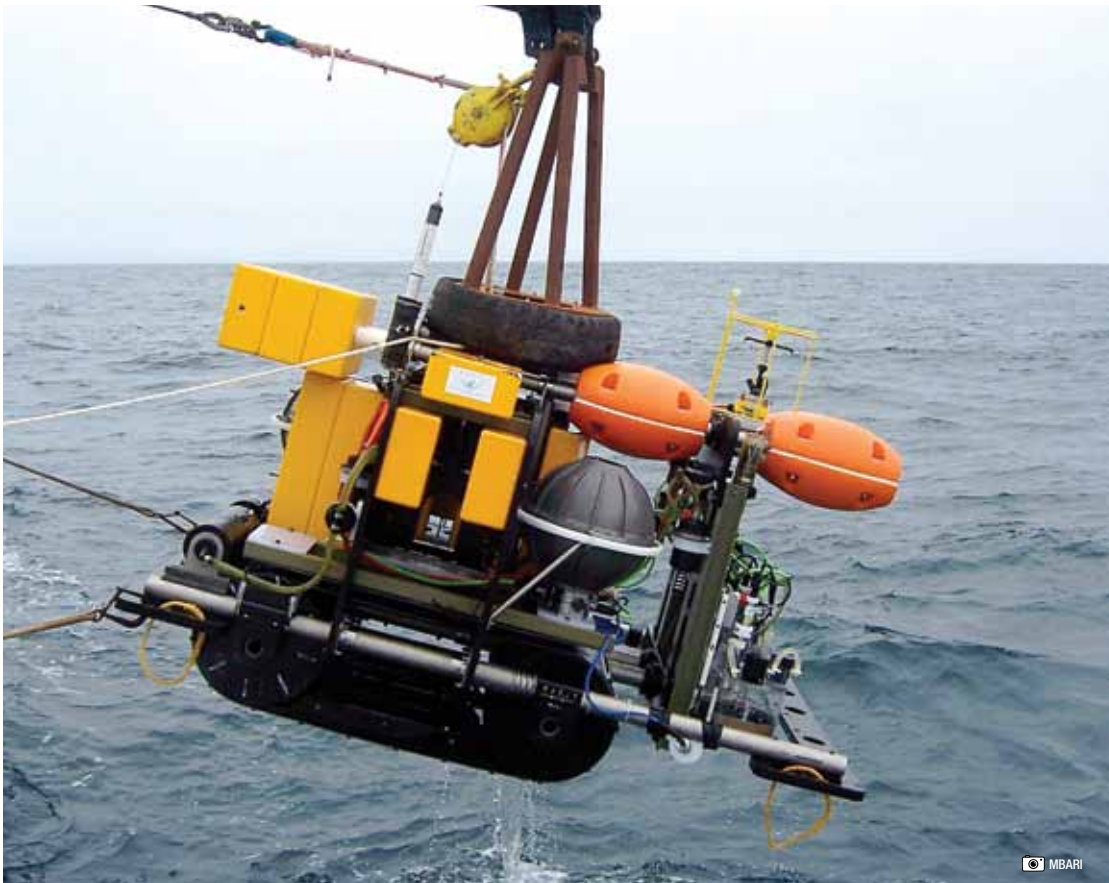


Figure 1: The Rover during recovery operations after a deployment in Monterey Bay.

be capable of changing its buoyancy by 113 kg during each deployment, which may last six months or more. To meet the depth and long mission length requirements, all one-atmosphere housings are made of titanium. Electrical equipment that can withstand ambient pressure, such as wiring and motors, is contained in lightweight Delrin plastic housings filled with Shell Tellus T 15 oil supplied by four separate positive-pressure oil compensation systems.

To traverse the seafloor, the Rover uses two 46 cm-wide spring-tensioned fibre-reinforced polyurethane lugged tracks that present a 0.94 m² footprint to support the Rover's in-water weight of 68 kg. This low surface-contact pressure (72 kg/m²) allows the Rover to move lightly over the sediment with minimal disturbance.

Two brushless propulsion motors (model EC 60, Maxon Precision Motors, Fall River, Massachusetts) are mounted at the rear of the chassis. Each motor drives a 308:1 reduction gearhead and is contained in an oil-filled housing. The motors are rated at 400 watts each, but they consume less than 100 watts during normal Rover operation. The gearhead output shafts are connected to the rear wheels via drive belts.

The Rover is 2.6 m long, 1.7 m wide, 1.5 m tall, and weighs 1136 kg in air. The vehicle frame is constructed of several 2.5 cm-thick black UHMW plates with grade 2 titanium pipes and brackets. Most of the 0.54 m³ of 625 g/L syntactic foam is in the form of 13 blocks, each having a volume of 28 L and rated for 6000 m depth. Six more "football" floats on the upper titanium tubes provide

additional flotation and can be adjusted fore and aft to trim the Rover's pitch.

At the front of the Rover are two respirometer racks. These are lead-screw-driven vertical carriages used to lower and raise the respirometer chambers. The two racks are completely independent to provide redundancy in case one system fails.

The 113 kg steel drop weight is suspended below the Rover's centre of gravity using a series of lever-arms that are retained by a redundant pair of standard burn wires (model C210-337-2, Teledyne Benthos, North Falmouth, Massachusetts). The Rover is ballasted to weigh 68 kg in water with the drop weight present, and to be 45 kg buoyant when the drop weight is released.

The 3 cm-diameter lift line for the Rover is attached to a titanium tube at the top of the vehicle between the two main bulkheads. To aid in recovery, the lift line is attached to a spar buoy with a 10 m-long polypropylene line. The spar buoy is a 6.5 m-long fiberglass and aluminum pole with a large football float in the middle and a steel weight at the bottom. The buoy is also equipped with a large flag, a VHF radio beacon, and a xenon flasher positioned almost 3 m above the water, greatly enhancing the visibility of the Rover during recovery operations.

Instrumentation

Like most underwater vehicles, the Rover platform exists to carry a suite of sensors. These instruments include:

- Benthic respirometers (2)
- Respirometer chamber cameras (2)

- Fluorometric cameras (2)
- Survey camera
- Current meter
- Guest instruments (up to 3)

Control and recovery of the Rover is aided by the following:

- Acoustic modem
- Argos satellite beacon
- VHF radio beacon
- Xenon flasher beacon

The Rover is primarily designed to measure sediment community oxygen consumption (SCOC). SCOC measurements are made using two respirometer chambers, each 30 cm in diameter and 20 cm deep (Figure 2). A Teflon-coated titanium cutting edge on the bottom of each chamber reduces insertion forces and minimizes the adhesion of sticky sediment. Dissolved oxygen in the enclosed water of each chamber is measured by an optode (model 3830, Aanderaa Data Instruments, Bergen, Norway), with a third optode mounted outside the chambers to provide reference measurements of ambient water.

Figure 2: The respirometer chambers on the front of the Rover.



Each chamber has three 7 cm-diameter valves on top that are opened while the chamber is inserted slowly at 5 mm/s, thus minimizing any “bow wave” effect and possible compression of the sediment to be studied. During respirometer incubations, the valves must remain tightly closed to minimize dissolved gas exchange with external water. The chamber valves are hydraulically actuated with water pressure produced by a pump (model 5T, Sea-Bird Electronics, Bellevue, Washington) on each chamber, feeding the three valves in series. These custom hydraulic valves consume much less power than a solenoid-actuated valve, and their slow operation minimizes any pressure disturbances.

A pair of crossed rods, rotated at 6 rpm by a small motor during respirometer incubations, circulates the water inside each chamber. Stirring is required to avoid stratification of oxygen-depleted water while avoiding sediment resuspension.

After each respirometer measurement, the chamber is extracted from the sediment. The valves are opened again during extraction to avoid suction effects. After extraction, a

cleaning pump sprays water across the interior surfaces of the chamber to remove adhering sediment that could affect subsequent measurements.

Two cameras (model Nova, Insite Pacific Inc., Solana Beach, California) mounted exterior to each chamber capture close-up images of the sediment inside the respirometers. These cameras have integral white LEDs to provide illumination. Images

are captured before chamber insertion to record any visible fauna present on the sediment, and after chamber insertion to verify insertion depth and chamber sealing.

Prior to the placement of the respirometer chambers, two fluorometric cameras (currently in development) will quantify the abundance, size, and distribution of phytodetritus on the sediment. Arrays of 460 nm blue LEDs will excite fluorescence in the phytodetritus, which will be imaged by two 1.4 megapixel monochrome cameras (model GC1380, Prosilica Inc., Burnaby, B.C., Canada). Light from the LED arrays will be blocked by 675 nm long-pass filters in front of each camera, allowing only the excited fluorescence to be recorded.

A 5 Megapixel color survey camera (model GC2450, Prosilica Inc.) is mounted at the front of the Rover and captures images every metre while transiting between measurement sites. These 50-degree-field-of-view oblique images provide a continuous record of the area traversed by the Rover, and aid in surveys of phytodetritus, megafauna, and structural sediment features. A single 250 W-s xenon strobe light (model YS-250Pro, Sea&Sea, Saitama, Japan) provides illumination for the survey camera.

An acoustic current meter (model 2D-ACM, Falmouth Scientific, Inc., Cataumet, Massachusetts), mounted at the top of the vehicle, measures current speed and direction for Rover navigation and provides a record of ambient conditions during deployment. A compass and tiltmeter are integrated into this unit and are used by the Rover to determine heading, and record pitch and roll.

The Rover can accommodate up to three guest instruments. The guest instrument ports supply switched power and an isolated RS-232 serial data connection. The power consumption and duty cycle of any guest instruments must be low enough to not adversely affect the energy remaining for other vehicle needs.

The Rover's acoustic modem (model ATM-887, Benthos, North Falmouth, Massachusetts) is a data telemetry modem that has been modified by Benthos to also provide a burn-wire output. The burn-wire is used to release the Rover's recovery drop weight, and the data telemetry channel is used to send commands and receive status during a mission.

To aid in locating the Rover once it returns to the surface after a mission, it carries a VHF radio beacon (model RF700A1, Novatech, Dartmouth, Nova Scotia), a xenon flasher (model ST-400A, Novatech), and an Argos satellite beacon (model AS900A, Novatech).

Electrical Design

The main vehicle computer (MVC) is housed in a 43 cm-diameter cast titanium sphere rated to a depth of 6000 m. The MVC is a PC/104 board stack consisting of four cards: an ARM9 computer card (model TS-7200, Technologic Systems, Fountain Hills, Arizona); a real-time clock daughter card (model TS-5620, Technologic Systems); a 12-port isolated serial card (model Xtreme/104 Isolated, Connect Tech, Inc., Guelph, Ontario); and a 5-port Ethernet switch (model PRV-1059, Parvus Corp., Salt Lake City, Utah). The TS-7200 was chosen primarily for its high performance-to-power-consumption ratio. The 200 MHz Cirrus ARM9 processor, 32 MB SDRAM, compact flash interface, and 10/100 Ethernet interface

deliver more than adequate computational performance while consuming only 2 Watts during operation, and less than 0.5 Watts while idling.

A network video server (model 241Q, Axis Communications, Lund, Sweden) captures images from the two chamber cameras and sends them via Ethernet to the MVC. The high-resolution survey camera is connected to the MVC via Ethernet directly.

Also housed in the same sphere are electronics for power conversion and switching. Two off-the-shelf serially controlled 8-channel relay boards (model CK1610, Carl's Electronics, Oakland, California) are used to switch power from the battery bus to all of the peripheral loads. This was a quick and inexpensive solution that enabled deployment and testing of the Rover; however, the cost of this short-term solution is wasted power, and no current, voltage, or ground-fault detection. Custom load controller boards are currently being designed that will have low quiescent power (a few mW), but are capable of providing up to hundreds of watts of galvanically isolated power at various voltages, and provide current and voltage monitoring, overcurrent protection, and ground fault detection. Until the load controllers are installed, the Rover has two DC-DC converters providing 5 VDC and 12 VDC (models UHE-5/5000-Q12 and UHE-12/2500-D24, Datel, Mansfield, Massachusetts) to loads that cannot operate directly from the 30 VDC bus.

All of the motors on the Rover, with the exception of the stirrer motors in the benthic respirometers, are brushless DC motors in oil-compensated housings. Attached to each oil-

filled motor housing is a small, hemispherical, one-atmosphere titanium pressure housing in which a motor driver/controller board (model EZSV23, All Motion, San Jose, California) is mounted. The motor controllers communicate with the MVC through an RS-485 multi-drop bus. The stirrer motors are brushed DC motors housed in Fluorinert.

Rover power for short deployments is provided by alkaline battery packs that are housed in a single separate 43 cm-diameter titanium sphere. These alkaline packs consist of 240 D cells, with multiple diode-isolated strings of 20 cells providing a nominal 2.9 kW-h at 30 VDC. For future long-term deployments, two spheres of lithium primary batteries will provide up to 19 kW-h of energy.

Software Design

A simple operational scenario consisting of four serial phases drove the requirements for the Rover control system. After an initial launch phase, the Rover executes multiple movement and measurement phases to accumulate data at different measurement sites. When completed, the system enters the recovery phase where it waits for an acoustic command to ascend to the surface. The design of the control system directly reflects this scenario with classes designed to manage each phase. A supervisor process controls the transitions between phases. The code for the phase objects is designed to run as separate execution threads, which are monitored by the control thread. Faults that occur during the execution of a phase are detected and trapped by the control thread, allowing the opportunity for recovery procedures to correct problems and perhaps continue with the mission.

The MVC runs a Linux 2.4-based operating system from Technologic Systems modified by MBARI to include the ConnectTech isolated serial card and the BusyBox command shell (www.busybox.net). The modular design of BusyBox resulted in a command shell tailored for use in the Rover and much smaller than a standard Linux shell environment.

The vehicle and instrument control applications are implemented in the Ruby programming language (www.ruby-lang.org). Ruby is a scripting language with many attributes of high-level languages that match-up well with rapid-development projects.

- Ruby is both object-oriented and dynamic, offering a high degree of flexibility.
- The interpreter is implemented in C, reasonably fast, and portable to many embedded systems.
- The concise syntax and powerful built-in features allow for quick application development and modifications.
- The threading and exception capabilities improve error handling, isolation, and recovery.
- Ruby applications are relatively simple and readable, making them more easily supported by non-programmers.
- Ruby does not require a tool-chain for the target system – modifications can easily be made while field testing.

The primary trade-off for these attributes is static, or compile-time, type-checking. Code compilation can greatly reduce run-time errors caused by using the wrong type of object in an expression. Since Ruby is a dynamic language, the type of object in any expression is not determined until run-time. This powerful

feature precludes static variable type checking and can result in run-time errors that are normally caught in more traditional languages during compilation. The Rover team chose to address this issue primarily by extensive testing of all mission scenarios using software simulation and hybrid hardware-in-the-loop tests. The software simulations test all of the control system by using software interfaces to all of the physical vehicle devices. These tests can be “warped” to run much faster than real-time and in batch mode, providing a regression-test framework that can be run on a workstation. The hybrid tests run on the vehicle and exercise the entire deployed system using real device interfaces. However, these tests can also use the warping technique to jump over non-dynamic portions of the mission. This technique reduces hardware-in-the-loop testing time by 90%, allowing potential errors to be observed and corrected quickly.

DEPLOYMENTS

Overview

Initial testing of the Rover’s ballast and trim was performed in MBARI’s 1.4 million litre saltwater test tank. The tank’s large size of 9 m width by 14 m length and 10 m depth provided enough volume to test the Rover’s drop weight release mechanism and the vehicle’s ability to move on the bottom.

The first at-sea testing took place from the R/V *Pt. Lobos* in Monterey Bay at a site about 40 km offshore and at a depth of 890 m, where the Rover was observed by the ROV *Ventana*. Subsequent dives at Station M, an abyssal area 220 km west of the central California coast, reached depths of over 4200 metres. These

deep dives were launched from the R/V *Atlantis* and observed by the DSV *Alvin*. Later dives at Station M were launched from the R/V *Western Flyer* and observed with the ROV *Tiburon*.

The purpose of the first dives was to test launch and recovery mechanisms and procedures, and to verify basic Rover movement on the seafloor. After an acceptable level of mechanical reliability was established, the instruments were added and tested as well.

Propulsion System

The tracks were observed to rest just on the sediment surface without sinking in, as was intended. However, sediment clinging to the track surface is carried forward on the top half of the tracks, acting as a conveyer belt, and dumped at the front of the vehicle near the respirometers. Stiff brushes added to the rear of the vehicle where the track leaves the seafloor have been effective in removing this sediment at the source.

Even with the brushes in place, simply moving too rapidly can kick up unacceptable quantities of sediment. In still water, Rover speeds above 2 cm/s were found to be too disruptive. When the Rover is moving into a current, higher speeds are possible. The vehicle chassis entrains some sediment-laden water during forward motion, and this water continues to move forward when the vehicle stops. If the ambient currents impinging on the front of the vehicle are too slow, then the disturbed sediment is deposited under the respirometer chambers, contaminating the study area. For this reason, the Rover's speed should not exceed that of the ambient water currents.

Sediment disruption is not the only consideration when choosing the Rover's speed. The Rover must move in the most energy-efficient manner to achieve the goal of operating longer than six months on a single set of batteries. If the speed is too low, movement to a new site takes a long time and a lot of power is consumed by the "hotel load," i.e. those loads such as the MVC, motor controllers, and cameras, which are using power but are not contributing to the vehicle's forward motion; only power consumed by the motors themselves does this. If the speed is too high, then hydrodynamic forces become large and power is wasted pushing through the water. Somewhere between these two extremes lies an optimum speed that minimizes total energy consumption.

To find this optimum speed, the Rover was operated in the test tank at various speeds while power consumption was monitored. These measurements are shown in Figure 3, along with a least-squares fit of a curve of the form

$$P_t(S_r) = P_h + C_f S_r + C_w S_r^2 \quad (1)$$

where P_t is the total power, S_r is the speed of the Rover, P_h is the hotel power, C_f is a constant that determines the power consumed by frictional forces in the drive mechanism, and C_w is a constant that determines the power consumed in pushing through the water.

The total energy consumed by a Rover movement is then the power consumption during the move multiplied by the time required for the move, i.e. the distance divided by the speed

$$E_t(S_r, D) = \frac{P_t(S_r) \cdot D}{S_r} \quad (2)$$

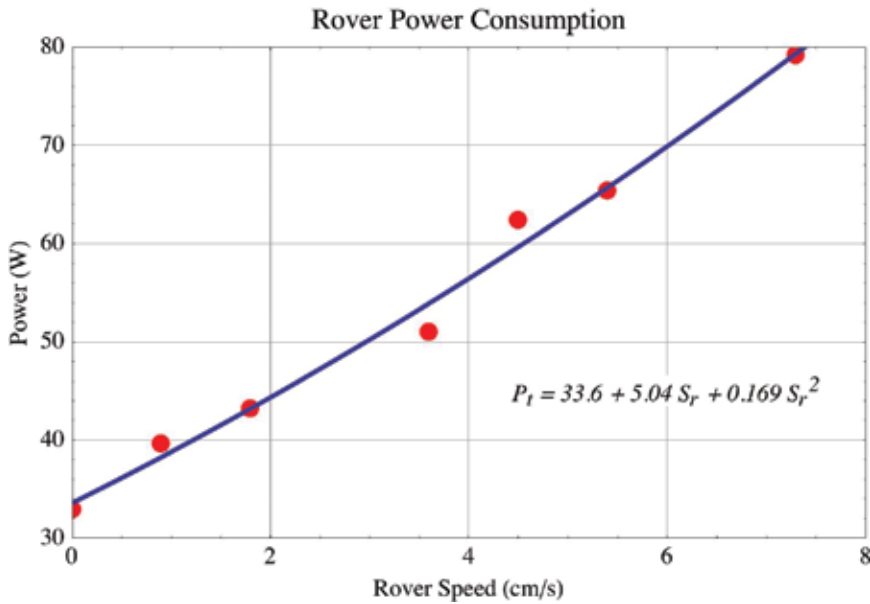
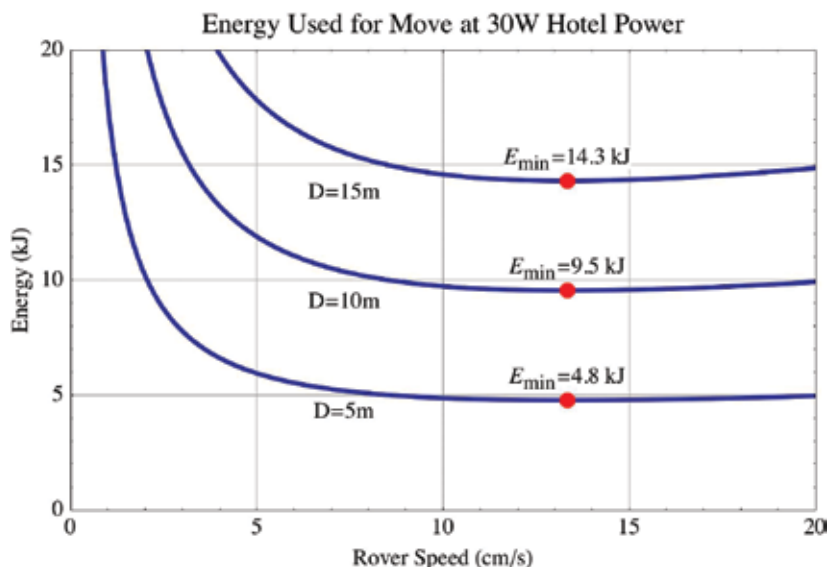


Figure 3: Measured power consumption as a function of speed.

where E_t is the total energy used for the move, and D is the distance travelled. Figure 4 shows the energy consumed as a function of Rover speed for three different distances with a hotel load of 30 W. The plots reveal that the least amount of energy is used under these conditions when the Rover moves at about 13.3 cm/s. It is also clear that for the range of speeds at which the Rover operates, the penalty for moving too slowly is much greater than that for moving too quickly. The minimum-energy speed does not vary with distance travelled; moving twice the distance takes twice the energy, but the conditions that determine the optimum speed remain unchanged.

Figure 4: Energy consumption as a function of speed at different transit distances.

A different perspective can be gained by varying the hotel load instead of the distance travelled. Figure 5 shows the energy consumed for a 10 m move as a function of Rover speed for three different hotel loads. The minimum-energy speed decreases with a reduction in the hotel load, as the penalty for moving slowly is less severe. The minimum-energy speed also becomes more critical as the hotel load is reduced, although the effect is not a large one.



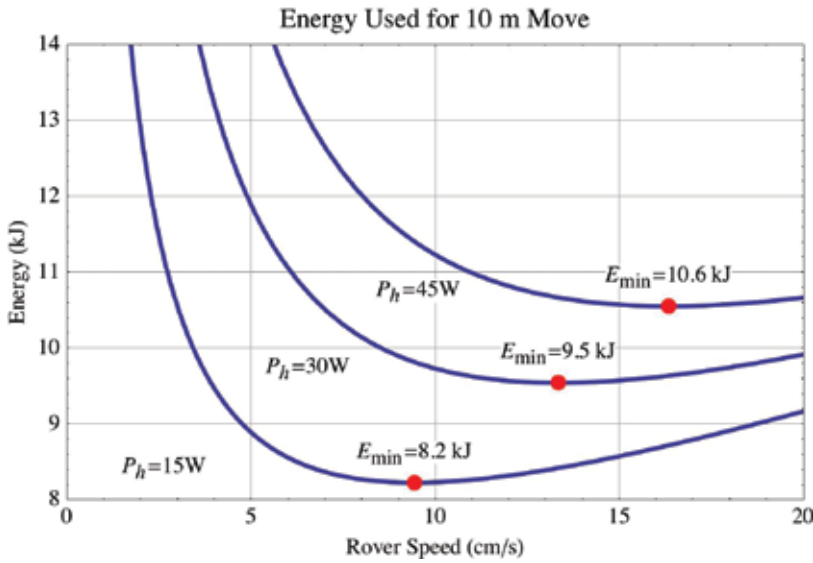


Figure 5: Energy consumption as a function of speed at different levels of hotel power.

The Rover will likely be restricted to speeds below 10 cm/s to avoid the problem of disturbed sediment. It is in this regime that the greatest gains from a reduction in hotel load can be realized. The current hotel load, exceeding 30 W, will certainly be reduced in the future by installing the custom load controller boards and by decreasing the clock speed of the MVC. If the hotel load can be reduced to around 15 W, then the cost of a 10 m move at 5 cm/s can be reduced from 12 kJ to less than 9 kJ – a savings of 25%.

The power analysis thus far has followed that of traditional free-swimming AUVs [Bellingham and Willcox, 1996; Willcox et al., 2001]. The Rover, however, is different in one important aspect: it

Figure 6: Energy consumption as a function of speed in still water and while driving into a current.

is not free-swimming and therefore its speed is restricted by conditions of the sediment and ambient bottom currents. Given that the Rover must always move against the current to carry away disturbed sediment, the energy cost of this current must be accounted for. Equation 1 can be modified to include a water current term that affects only the hydrodynamic forces

$$P_t(S_r, S_w) = P_h + C_f S_r + C_w(S_r + S_w)^2 \quad (3)$$

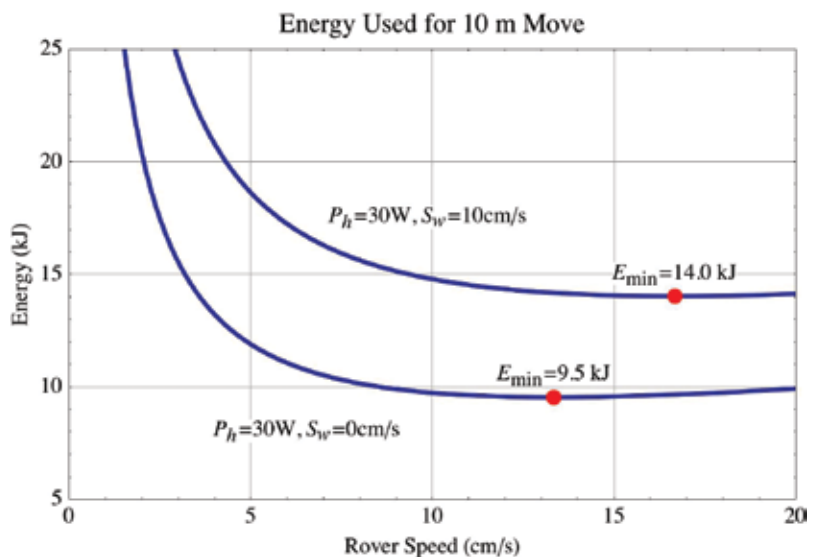




Figure 7: Images of the sediment beneath the respirometer chambers (port on left, starboard on right) before and after chamber insertion at 896 m in Monterey Bay.

where S_w is the speed of the water current. Figure 6 uses this new power equation to show the energy consumed for a 10 m move as a function of Rover speed in both still water and with a head current of 10 cm/s. As expected, moving into a current increases energy consumption at a given Rover speed. However, the current is not necessarily disadvantageous for the Rover's energy consumption. In still water, the Rover is restricted to speeds of around 2 cm/s, at which about 20 kJ of energy are expended for a 10 m move. With a 10 cm/s current, the Rover can move at higher speeds without contaminating the study area. If, for instance, the Rover moves at 9 cm/s into a 10 cm/s head current, it expends about 15 kJ for the same 10 m move – a savings of 25% compared to a move with no current. Further gains may perhaps be realized by moving obliquely to the current, where most of the sediment-clearing effects of the current are retained without incurring the full hydrodynamic drag penalty.

Imaging System

The images from the respirometer chamber cameras are 640-line still captures from small NTSC video cameras. While these images are fairly low resolution, they provide enough information to determine if the chambers are inserted, how far they are inserted, and if there are any

anomalous fauna inside the chambers (e.g. Figure 7) that will affect the oxygen consumption. To help quantify the spatial distribution of macro fauna along the 10 m transits between respirometer sites, still images from the survey camera are analyzed and optionally stitched together to form a linear mosaic (Figure 8).

Benthic Respirometer Measurements

Only minor problems were encountered during testing of the respirometers. On one early dive, the switch that senses when the chamber is inserted to the correct depth into the sediment got stuck and did not activate. As a result, the chamber kept going until the rack limit switch was activated, and no damage was done. Had the rack limit switch failed, the motor controller overcurrent sensor would have tripped, protecting the motor and the rack. This was a good demonstration of the Rover's layered structure, where systems are expected to eventually fail and other systems, hopefully seldom-used, activate to prevent disaster.



With the racks working, reliable respirometer measurements could be made. A typical SCOC measurement recorded at 890 m in Monterey Bay is shown in Figure 9. The reference optode shows more than $6 \mu\text{M}$ of variation in dissolved oxygen concentration over the 17 hours of the record. The chamber optode, however, shows a steady decrease in oxygen due to the respiration of organisms in the sediment. The slope of the chamber optode curve, which here is about $-0.3 \mu\text{M}/\text{hour}$, is an indicator of biological activity. SCOC measurements must be stopped before oxygen levels get prohibitively low, causing unnatural conditions.

One of the distinguishing features of the Rover is its ability to take duplicate respirometer incubations in multiple locations during a single deployment. Figure 10 shows the first three incubations taken during a deployment in Monterey Bay. The second and third show the expected negative linear slope characteristic, but the first incubation shows an initial *increase* in oxygen concentration. This is a known feature of these instruments, and is due to trapped air in the respirometer chamber. Although the chamber valves are opened soon after the Rover enters the water, it is impossible to release all of the air in the chambers. Small bubbles get trapped in the stirring motor assembly, and the acrylic chambers themselves may absorb some oxygen [Carignan et al., 2007]. This excess oxygen is then released slowly into the chamber, affecting the first couple of incubations.

Figure 8: A photo mosaic compiled from nine consecutive survey camera images. The images were captured at one-metre intervals as the Rover transited to a new measurement site at 896 m in Monterey Bay.

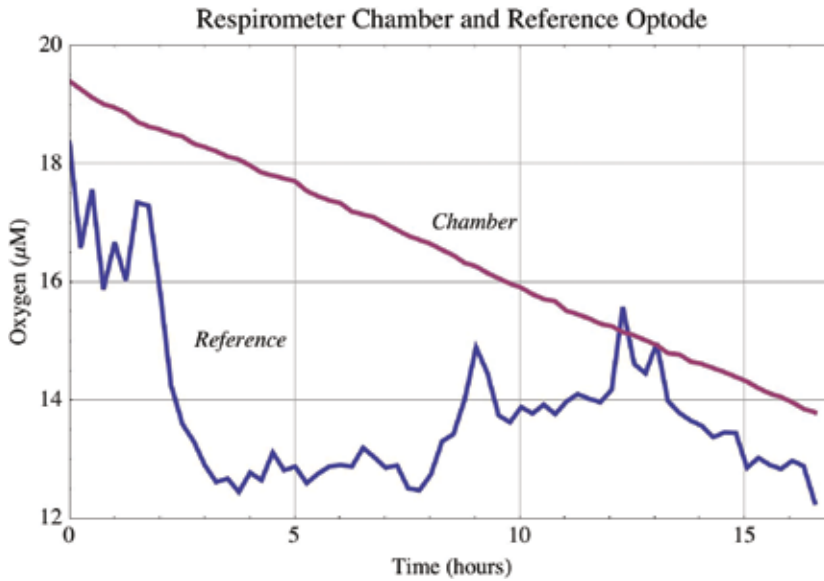


Figure 9: Oxygen measurements in Monterey Bay from inside a respirometer chamber and from a reference optode outside of the chamber.

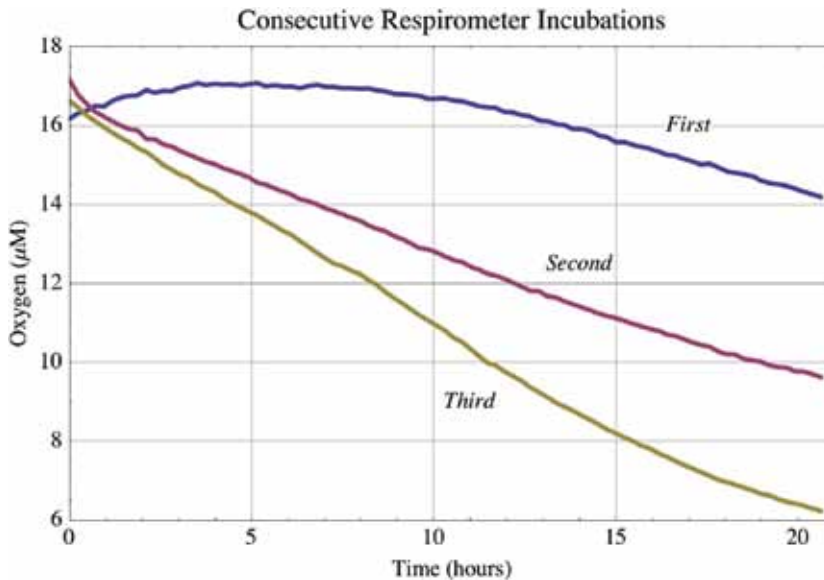


Figure 10: The first three respirometer incubations of a deployment in Monterey Bay.

One strategy for dealing with this effect is to simply discard the first incubations, knowing that they do not represent natural conditions. However, a closer examination of the first incubation can reveal some useful insights. Figure 11 shows the first curve of Figure 10 on an expanded scale. The change in oxygen concentration represented by these data points can be modeled by a curve of the form

$$O_2(t) = O_{2amb} + O_{2bub}(1 - e^{-t/\tau}) - (K \cdot t) \quad (4)$$

where O_2 is the oxygen concentration, O_{2amb} is the initial ambient oxygen concentration when the chamber is closed, O_{2bub} is the total increase in oxygen concentration due to the trapped air, τ is the time constant for the release of the trapped oxygen, and K is the rate of decrease in oxygen concentration due to consumption by the sediment community. A

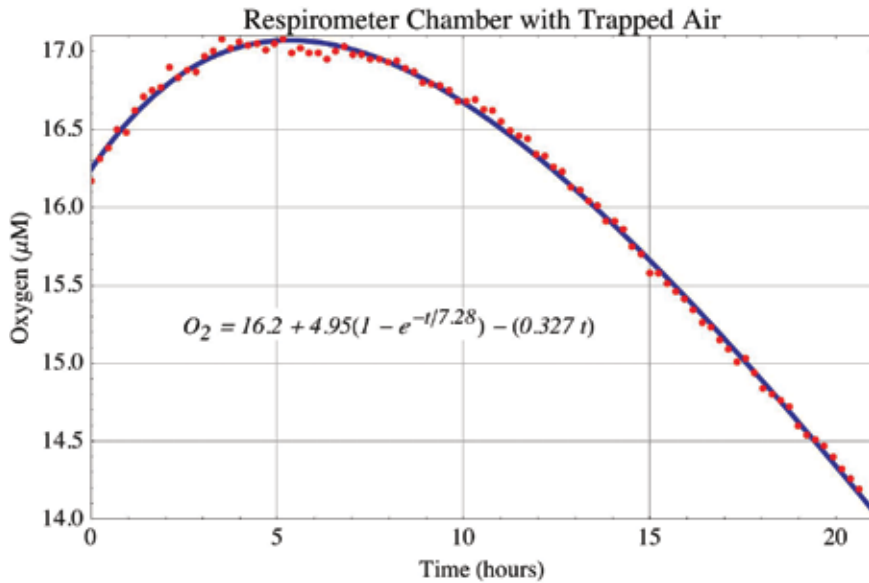


Figure 11: Data from the first respirometer incubation in Figure 10, showing the effects of trapped air in the chamber.

least-squares fit of this curve to the data points yields the parameters shown in the figure.

These parameters indicate that the ambient oxygen concentration, O_{2amb} , was $16.2 \mu\text{M}$, and that the oxygen released from the trapped air would have caused an increase in concentration, O_{2bub} , of $4.95 \mu\text{M}$ if no oxygen consumers were present. Knowing the value of O_{2bub} enables us to calculate the volume of the bubble, at 1 atmosphere, that released this oxygen. Since the volume of the chamber inserted into the sediment is 9.0 L , we know that the total amount of oxygen released is

$$9.0 \text{ L} \cdot 4.95 \frac{\mu\text{Mole}}{\text{L}} = 45 \mu\text{Mole} \quad (5)$$

One mole of oxygen, or any gas, is 22.4 L at STP, but air is only 21% oxygen, so the size of the bubble at STP that would contain $45 \mu\text{Moles}$ of oxygen is

$$45 \mu\text{Mole} \cdot 22.4 \frac{\text{L}}{\text{Mole}} \cdot \frac{1}{0.21} = 4.8 \text{ mL} \quad (6)$$

suggesting that a relatively small volume of air trapped at the surface can have a large effect on the first measurements made at depth.

The value of τ in Figure 11 suggests that it takes 7.28 hours for 67% of the oxygen from the bubble to be released into the chamber. After three time constants, or about 22 hours, less than 5% of the oxygen in the bubble remains.

Finally, the value of K suggests that oxygen is being consumed at a rate that causes the concentration to fall by $0.327 \mu\text{M}/\text{hour}$. This consumption rate could have been estimated by disregarding the first part of the curve and calculating the slope of only the last part, but by fitting the model to the whole measurement, more data are used and a more accurate result is obtained.

Note that the middle term in Equation 4 is empirically derived and may not represent the physics of the oxygen release mechanism. The actual rate of oxygen release is a complex

function depending, among other things, on the surface area of the gas-water interface, which in turn depends on the unknown shape of the bubble or bubbles [Leifer et al., 1995]. Some of the oxygen may be released from the acrylic chamber walls, which would have to be described in a different manner. In any case, the model is useful as it allows us to understand the quantities and time periods involved, and yields valid SCOC measurements from otherwise compromised data.

CONCLUSIONS AND FUTURE WORK

Initial deployments of the Rover have been very successful. Thanks to the excellent vantage points provided by the ROVs *Ventana* and *Tiburón*, and DSV *Alvin*, numerous minor problems have been identified and addressed.

An analysis of the Rover's power use leads us to the somewhat surprising conclusion that energy can be saved by driving into a current. This knowledge will be incorporated into the vehicle software and will result in longer missions and more science data. Analysis of the respirometer chamber data shows that the Rover can make valid measurements of SCOC, and that the excess oxygen in the chambers can be accounted for by trapped air.

In the coming year, the fluorometric imaging cameras will be built and tested. The Rover will also be connected to the Monterey Accelerated Research System (MARS) cable for further testing in Monterey Bay (www.mbari.org/mars). The MARS cable will provide a continuous power and data connection from shore to the Rover, which will greatly facilitate the development of the Rover's autonomous software.

REFERENCES

- Bellingham, J. and Willcox, J. [1996]. *Optimizing AUV oceanographic surveys*. (Proceeding of IEEE Symposium on Autonomous Underwater Vehicle Technology, Monterey, California, pp 391-398.)
- Carignan, R., St-Pierre, S., and Gachter, R. [2007]. Use of diffusion samplers in oligotrophic lake sediments: Effects of free oxygen in sampler material. *Limnology and Oceanography*, Vol 39, No 2, pp 468-474.
- Leifer, I., Asher, W., and Farley, P. [1995]. *A validation study of bubble mediated air-sea gas transfer modeling for trace gases*. (Proceedings of the Third International Symposium on Air-Water Gas Transfer Heidelberg University, Eds. B. Jahne and E.C. Monahan, Aeon Verlag, Hanau, Germany, pp 269-283.)
- Smith Jr. K.L., Glatts, R.C., Baldwin, R.J., Beaulieu, S.E., Uhlman, A.H., Horn, R.C., and Reimers, C.E. [1997]. An autonomous, bottom-transecting vehicle for making long time-series measurements of sediment community oxygen consumption to abyssal depths. *Limnology and Oceanography*, Vol 42, pp 1601-1612.
- Smith Jr. K., Baldwin, R., Karl, D., and Boetius, A. [2002]. Benthic community responses to pulses in pelagic food supply: North Pacific Subtropical Gyre. *Deep-Sea Research Part I – Oceanographic Research Papers*, Vol 49, pp 971-990.
- Smith Jr. K.L. and Baldwin, R.J. [1983]. Deep-sea respirometry: In situ techniques. E. Gnaiger and H. Forstner [eds.], *Polarographic oxygen sensors: aquatic and physiological applications* (pp 298-319). Berlin, Heidelberg, New York: Springer.

- Smith Jr. K. and Kaufmann, R. [1999]. Long-term discrepancy between food supply and demand in the deep Eastern North Pacific. *Science*, Vol 284, pp 1174-1177.
- Tengberg, A. et al. [2005]. Intercalibration of benthic flux chambers II. Hydrodynamic characterization and the flux comparisons of 14 different designs. *Marine Chemistry*, Vol 94, pp 147-173.
- Willcox, J., Bellingham, J., Zhang, Y., and Baggeroer, A. [2001]. Performance metrics for oceanographic surveys with autonomous underwater vehicles. *IEEE Journal of Oceanic Engineering*, Vol 26, No 4, pp 711-725.